Cubic–tetragonal phase transition in $Ca_{0.04}Sr_{0.96}TiO_3$: a combined specific heat and neutron diffraction study

Cubic–tetragonal phase transition in $Ca_{0.04}Sr_{0.96}TiO_3$: a combined specific heat and neutron diffraction study

M C Gallardo[1], **A I Becerro**[2], **F J Romero**[1], **J del Cerro**[1], **F Seifert**[3] and **S A T Redfern**[4]

[1] Departamento de Física de la Materia Condensada, Instituto de Ciencia de Materiales de Sevilla, Universidad de Sevilla–CSIC, PO Box 1065, 41080 Sevilla, Spain
[2] Departamento de Química Inorgánica, Instituto de Ciencia de Materiales de Sevilla, Universidad de Sevilla–CSIC, Avenida Américo Vespucio s/n, 41092 Sevilla, Spain
[3] Bayerisches Geoinstitut, Universität Bayreuth, 95440-Bayreuth, Germany
[4] Department of Earth Sciences, University of Cambridge, Downing Street, Cambridge CB2 3EQ, UK

E-mail: mcgallar@us.es

Abstract
The specific heat corresponding to the tetragonal-to-cubic transition in $Ca_{0.04}Sr_{0.96}TiO_3$ perovskite has been measured by conduction calorimetry. The order parameter of the transition has been obtained by means of neutron diffraction at low temperatures. Comparison of calorimetric data with the evolution of the order parameter indicates that this transition seems to follow a mean field Landau potential as in $SrTiO_3$. The linear behaviour of the excess of entropy versus temperature suggests that a 2–4 Landau potential is sufficient to describe the transition.

1. Introduction

For many years, phase transitions in ABO_3 perovskites (A = Na, K, Ba, Sr, Ca, Pb, La, etc, B = Nb, Ta, Ti, Zr, Al, etc) have received wide attention. They are employed as textbook illustrations of structural phase transitions [1]: many of these perovskite materials are cubic above a critical temperature at normal pressures and some of them undergo a variety of temperature-induced structural phase transitions [2–4]. Perovskites display a variety of electronic properties, from the ferroelectricity of $BaTiO_3$ [5] and the superconductivity of $Ba(Bi_{1-x}Pb_x)O_3$ [6] to the magnetoresistivity of $(La_{1-x}Ca_x)MnO_3$ [7]. In addition, the Earth's lower mantle is believed to be composed mainly of $MgSiO_3$-rich perovskite, and the understanding of the temperature-and pressure-induced phase transitions in this structure may be of crucial importance in appreciating the geophysical properties of the lower mantle, especially near its base.

In all these areas of research, the influence of dopants, in either the A or the B cation sites of the perovskite structure, is of interest. The system $CaTiO_3$–$SrTiO_3$ provides an example of a continuous solid solution with cation substitution, Ca for Sr, on the A site. The Sr-rich end-member is cubic at room temperature, with space group $Pm\overline{3}m$ [8]. It exhibits an antiferrodistortive phase transition (from cubic ($Pm\overline{3}m$) to tetragonal ($I4/mcm$) symmetry) at 105 K, which results from the freezing of one of the triply degenerate R_{25} modes in which adjacent octahedra vibrate about one of the cubic [100] axes [9]. Studies on Ca-doped $SrTiO_3$ have shown that the antiferrodistortive transition temperature is strongly dependent on composition, even at extremely low Ca contents. Bianchi *et al* [10] have found that the antiferrodistortive transition for the member $Ca_{1-x}Sr_xTiO_3$ with $x = 0.993$ occurs at 125 K while Guzhav *et al* [11] have reported a transition temperature of 148 K for $x = 0.986$. A detailed study on the Sr-rich end of the solid solution below room temperature by Becerro *et al* [12] has shown that the cubic-to-tetragonal phase boundary shows a markedly non-linear behaviour in contrast to the quasi-linear variation of the boundary at lower Sr contents [13]. This behaviour is due to quantum fluctuations, which enhance the stability of the high-symmetry phase, reducing the observed transition temperature [14].

Regarding the thermodynamic behaviour, we have recently shown that the cubic–tetragonal phase transition in pure $SrTiO_3$ follows mean field Landau behaviour, rather than a Heisenberg model as previously believed [15]. We concluded that this transition is near to the tricritical point and the coefficients of the corresponding 2–4–6 Landau potential were reported.

The aim of the present paper is to ascertain whether or not the antiferrodistortive phase transition in Ca-doped $SrTiO_3$ can also be described effectively using the Landau theory. It is also important to know whether calcium defects induce fluctuations that cause deviations from mean field behaviour, and whether the phase transition is of the same character as in pure $SrTiO_3$. With that in mind, we have selected the $Ca_{0.04}Sr_{0.96}TiO_3$ composition because it has a significant calcium content, aiding comparison with the end-member. Furthermore, it displays the cubic–tetragonal transition at a temperature which is inside the temperature range of our calorimeter. We have recently demonstrated [16] that in order to obtain reliable conclusions about the behaviour of phase transitions, it is necessary to analyse the correlation of the order parameter with the transition excess entropy. Otherwise, the study of just one physical parameter near the transition point might yield erroneous results. Following this observation, the present study has been accomplished by combining two complementary techniques: calorimetric measurements have provided the entropy excess of the transition while *in situ* neutron diffraction measurements have been used to obtain the temperature dependence of the driving order parameter.

2. Consequences of Landau potential

According to the classical Landau theory of phase transitions, the excess free energy due to the transition in a single domain is

$$\Delta G = \tfrac{1}{2}A(T - T_c)Q^2 + \tfrac{1}{4}BQ^4 + \tfrac{1}{6}CQ^6 + \cdots. \tag{1}$$

This expression leads to a continuous phase transition for A, B, C all positive. Furthermore, one of B and C is usually small enough (relative to the other) to be neglected. If $B \gg C$ we obtain a second-order phase transition with a (2:4) Landau potential. If the phase transition is near to the tricritical point, as in the case of $SrTiO_3$, neither B nor C can be neglected.

The specific heat excess due to a phase transition is

$$\Delta c_p = -T\left(\frac{\partial^2 \Delta G}{\partial T^2}\right)_{Q=Q_{equilibrium}} \qquad \text{at } T_c; \qquad \frac{\Delta c_p}{T_c} = \frac{A^2}{2B}; \qquad (2)$$

in both cases (2–4 or 2–4–6 Landau potential) since the temperature dependence is only in the first term, and the ratio $\Delta c_p/T_c = A^2/2B$ must be constant, if the same kind of transition takes place.

On the other hand, in a 2–4 Landau potential, we have the relationship

$$\Delta S = \left(\frac{\partial \Delta G}{\partial T}\right)_{Q=Q_{equilibrium}} = \frac{1}{2}A Q^2_{equilibrium}. \qquad (3)$$

The excess entropy ΔS is expected to be proportional to the square of the order parameter Q for any behaviour described by a Landau potential like equation (1). This particular relation between entropy and order parameter is in principle broken in the asymptotic regime for all other universality classes [16]. Its experimental checking can thus be an effective way to distinguish between genuine fluctuation-driven critical behaviour and pure Landau behaviour.

Comparison of the order parameter with that of the excess entropy is therefore a convenient way to determine whether a given phase transition follows the predictions of Landau theory, or of some other critical model. The experimental technique is to measure some experimental quantity that scales in a known way with the order parameter as a function of temperature, and compare these data with calorimetric measurements of the excess entropy. In this way, we may test whether or not the proportionality implied by equation (3) is obeyed. By analysing distinct sets of experimental data for a given phase transition, we have a much more reliable test of the behaviour of a material.

Thus in a 2–4 Landau potential:

$$\Delta S = \frac{A^2}{2B}(T - T_c);$$

so the slope of the excess of entropy versus temperature gives also the relation $A^2/2B$.

3. Experimental details

$Ca_{0.04}Sr_{0.96}TiO_3$ was synthesized by drying $CaCO_3$ (Chempur, 99.9%) and $SrCO_3$ (Aldrich, 99.999%) at $500\,°C$ and TiO_2 (Aldrich, 99.9%) at $1000\,°C$ for 3 h. The mixture of the stoichiometric amounts was heated to $1300\,°C$ at a rate of $20\,°C\,h^{-1}$ and kept at that temperature for 4 h. After grinding in an agate mortar, the sample was fired in air at $1600\,°C$ for 48 h with periodic regrinding, and finally rapidly cooled. Analysis by microprobe showed it to be close to the nominal composition with $Sr/(Sr+Ca) = 0.958(17)$ and homogeneous at the 1% level. The powder was pressed and sintered at $1600\,°C$ for 24 h to produce three pellets of 9 mm diameter $\times$ 3 mm height.

Neutron powder diffraction patterns were recorded using the two-axis diffractometer D1B at the Institut Laue-Langevin, Grenoble, France. The instrument is equipped with a position-sensitive detector of 400 cells, which span $80°$ in 2θ. Neutrons of wavelength 2.52 Å were used, which give the highest neutron flux and a range of adequate scattering vectors. The pellets were contained in a 10 mm diameter $\times$ 70 mm open-ended vanadium sample can which was connected to the centre stick of a standard cryostat. The sample was cooled down to 20 K and then heated up at $1\,K\,min^{-1}$. Diffraction patterns were recorded continuously every 5 min while heating up to room temperature. A total of 60 diffraction patterns were obtained as a function of temperature.

For the measurements of specific heat and latent heat, we used an original experimental system developed and built by ourselves, which uses the conduction calorimetry method (also known as microcalorimetry), and is fully described elsewhere [17, 18]. This technique is based on the measurement of heat flux. The sample is placed between two identical fluxmeters, each formed of a large number of thermocouples placed electrically in series and thermally in parallel [19]. Using this method, it is possible to obtain absolute values of the specific heat of the sample. In addition, the heat flux exchanged by the sample, which gives the total enthalpy change during the transition, has been measured using a technique analogous to differential thermal analysis [20]. The measurements of specific heat and heat flux are made in independent experiments, but using the same calorimeter and sample, and under the same thermal conditions. Thus it is possible to directly compare the results of the two experiments. The measurements were carried out cooling the sample from room temperature in quasi-static conditions, at a constant rate of 0.2 K h^{-1}. As each measurement of specific heat takes 20 min, we have a point each 0.07 K approximately. The transition entropy excess is obtained by the integration of the transition specific heat excess. The analysis of ΔS, instead of checking directly the expected critical behaviour of the excess specific heat Δc, has the fundamental advantage of using an integrated quantity with a smooth temperature dependence that is independent of experimental statistical errors in the measurement of Δc.

4. Results

4.1. Neutron diffraction study

As it lies near the Sr-rich end-member of the $CaTiO_3$–$SrTiO_3$ solid solution, $Ca_{0.04}Sr_{0.96}TiO_3$ is expected to transform from cubic ($Pm\bar{3}m$) to tetragonal ($I4/mcm$) symmetry with decreasing temperature below RT. The decrease in symmetry from $Pm\bar{3}m$ ($a^0a^0a^0$) to $I4/mcm$ ($a^0a^0c^-$) is due, mainly, to the tilting of successive octahedra along the [001] axis in opposite senses about that axis (as indicated by the negative superscript in Glazer's notation [21]). Figure 1 shows the neutron diffraction patterns of the sample recorded between 35° and 115° 2θ at both ≈RT (while heating up from 315 to 320 K) and low temperature (while heating up from 20 to 25 K). The low-temperature pattern exhibits all the reflections expected for the tetragonal $I4/mcm$ space group. Both 211 and 213 are superlattice reflections which arise due to the antiphase tilting while the rest correspond to the main perovskite sublattice reflections. With increasing temperature, the intensity of both of the superlattice reflections decreases until they simultaneously disappear at ∼225 K. The RT pattern in figure 1 displays, exclusively, the main perovskite reflections, which can be indexed in the cubic $Pm\bar{3}m$ space group.

It is well known that the order parameter Q of a transition describes the deviation of the low-temperature phase from that of the high-temperature phase. A way of experimentally measuring the order parameter variation is provided through the general relationship $\langle Q \rangle^2 \propto I_k$, where I_k is the intensity of a superlattice reflection, which appears as a consequence of the transition [22]. Figure 2 shows the variation with temperature of the square of the observed structure factors (directly proportional to the intensity) of both the 211 and 213 reflections. These have zero intensity under $Pm\bar{3}m$ symmetry and become non-zero below the $Pm\bar{3}m \rightarrow I4/mcm$ transition. The low intensity shown by both superlattice reflections, even at the lowest temperature, gives a high data scatter, and hence the data in figure 2 have been binned according to temperature. The pattern of intensity behaviour in the whole temperature range is similar for both reflections: it shows zero value from RT down to ∼235 K and then increases almost linearly to ∼115 K. Below this temperature the rate of change of superlattice

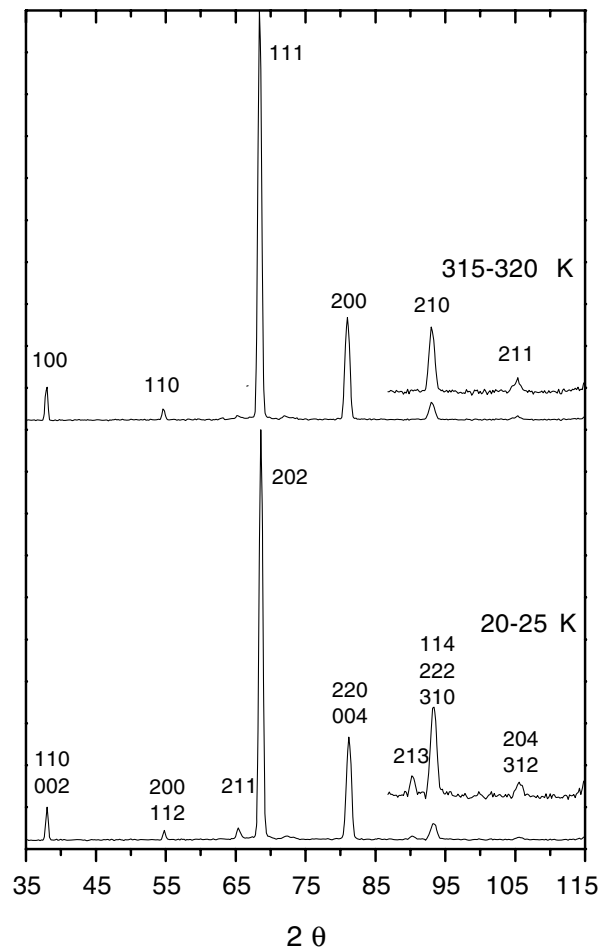**Figure 1.** Neutron diffraction patterns ($\lambda = 2.52$ Å) of Ca$_{0.04}$Sr$_{0.96}$TiO$_3$ perovskite recorded while heating up from 20 to 25 K and from 315 to 320 K at a heating rate of 1 K min^{-1}.

intensity decreases on cooling, so the temperature dependence becomes flatter closer to 0 K. By making an analogy with similar systems, we interpret this as the influence of quantum saturation effects. It is not possible to give a definitive saturation temperature for the data, other than to say that the departure from linearity occurs at temperatures lower than around 115 K.

4.2. Calorimetric study

The measured specific heat of Ca$_{0.04}$Sr$_{0.96}$TiO$_3$, from 170 to 260 K, is represented in figure 3. Directly from this graph, we see that the shape of the anomaly in the specific heat is very rounded, and it extends over a wide range of temperature. The exact transition temperature, as the maximum of specific heat, is therefore difficult to determine from this graph. This shape may be caused by slight inhomogeneities in the Ca distribution, as this would cause the transformation temperature to vary across the sample. Due to the fact that we use a power sample, the influence of crystalline surfaces would lead to a similar effect. In spite of this,
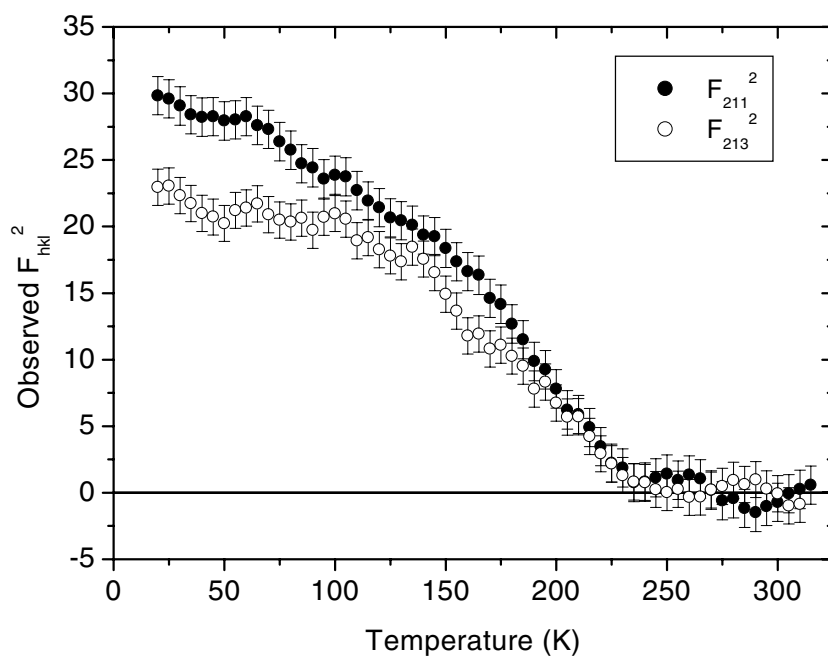
Figure 2. Variations in intensity of the 211 and 213 reflections with increasing temperature. The data are smoothed by adjacent averaging of three points.
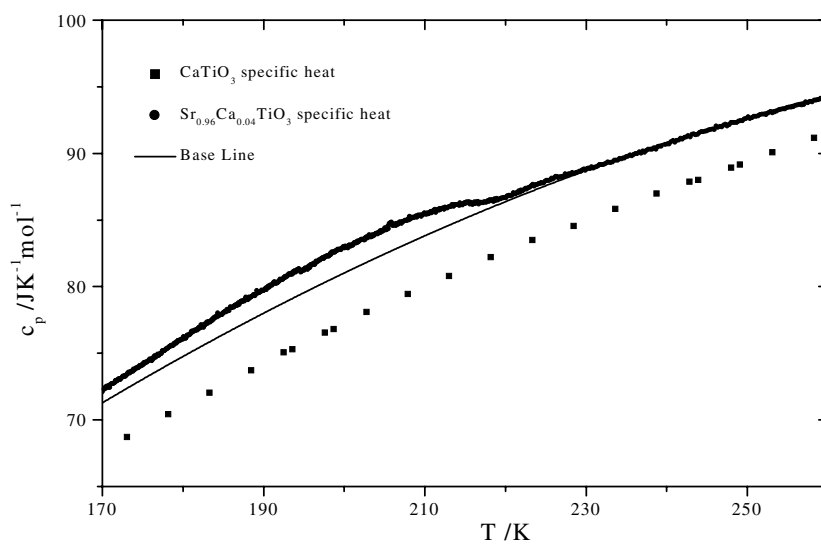

Figure 3. The specific heat of $CaTiO_3$ (filled squares) between 170 and 260 K from [23]: experimental data for the specific heat of $Ca_{0.04}Sr_{0.96}TiO_3$ (fill circles). These data have been obtained by conduction calorimetry, cooling the sample at a constant rate of 0.2 K h^{-1}. The baseline considered (continuous curve) for this phase transition (see the text) is the second-order polynomial $c = aT^2 + bT + e$ and $a = -0.001\,14$ J mol^{-1} K^{-3}, $b = 0.7474$ J mol^{-1} K^{-2}, $e = -22.7676$ J mol^{-1} K^{-1}.
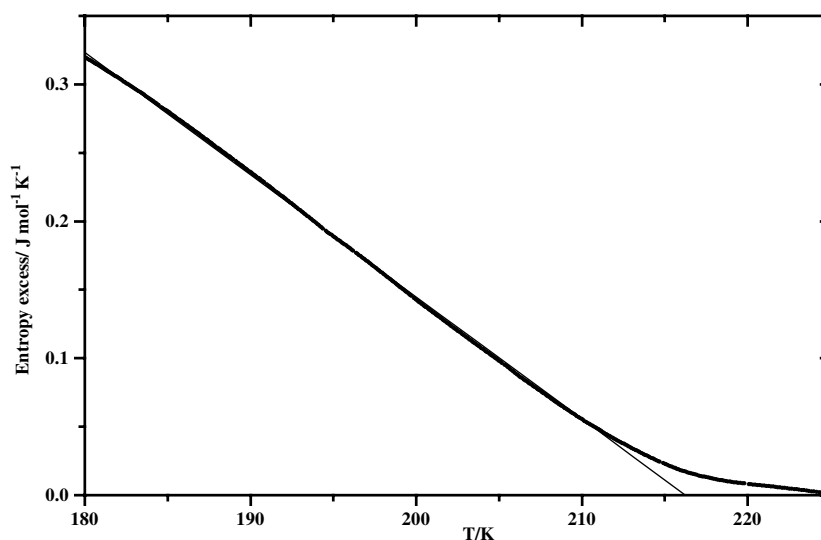
Figure 4. The temperature evolution of the excess entropy obtained by integration of the specific heat excess. The temperature range is from the transition temperature down to 30° below. The straight line adjusted to the data is $\Delta S = a + bT$ and $a = 1.925(3)$ J mol^{-1} K^{-1}, $b = -0.0088(2)$ J mol^{-1} K$^{-2} = A^2/2B$ corresponding to a 2–4 Landau potential.

we estimate 220 K for the transition temperature, as shown by the onset of the specific heat excess.

In order to obtain the specific heat excess we must evaluate the baseline for the specific heat curve. From just the specific heat graph, we cannot establish whether the lower data at 170 K still have a contribution from the singular part of the specific heat or whether they have reached the baseline.

On the other hand, from figure 2 it is difficult to determine where quantum saturation starts, but this is clearly below 170 K. Thus, at this temperature there must be some variation of the entropy, so at this temperature there is still specific heat excess, but, *a priori*, we cannot know how much.

At this point we cannot use the traditional way to determine the baseline. To solve this problem, we take reliable data on the specific heat of $CaTiO_3$ [23] that is a similar material and does not have any anomaly in the temperature range that we are analysing in $Ca_{0.04}Sr_{0.96}TiO_3$. These specific heat data are also represented in figure 3. From this graph we can see that up to 220 K the shapes of the two curves for the specific heat are the same; the only difference is a translation in the absolute value of the specific heat. This suggests that we can take the translated curve from $CaTiO_3$ as the baseline for $Ca_{0.04}Sr_{0.96}TiO_3$. The procedure is to fit a second-order polynomial to the $CaTiO_3$ specific heat data and translate it until it coincides with the $Ca_{0.04}Sr_{0.96}TiO_3$ specific heat data up to 220 K; this polynomial is also represented in figure 3. We must point out that the translation only represents 2% of the specific heat absolute value and may be due only to the different calorimetric technique used for the measurement of the specific heat.

The analysis of the heat flux does not give any significant anomaly around the transition temperature, from which we may conclude that the phase transition is second order [20].

In order to compare these results with those on the temperature dependence of the order parameter, the entropy excess has been calculated by integration of the specific heat excess
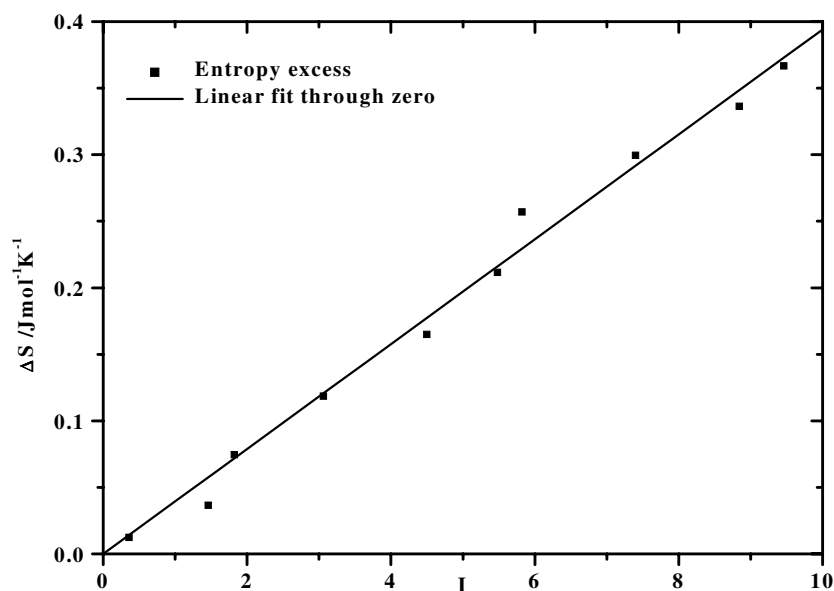
Figure 5. The correlation between the excess entropy and the excess intensity of neutron diffraction experiments. The straight line through zero adjusted to the data is $\Delta S = bI$ (I in arbitrary units) and $b = 0.0394(9)$ arbitrary units.

data. Figure 4 shows the entropy excess in a temperature range that spans 30° below the transition temperature. The entropy excess shows, in this interval, an almost linear behaviour, as was observed in the plot of the intensity of the tetragonal superlattice reflections versus temperature over the same temperature range.

4.3. Comparing calorimetric and diffraction data

Differences in thermometer calibration and in scanning rates used in the calorimetry and in the neutron diffraction measurements may explain the different transition temperatures indicated by the two methods (220 versus 235 K). In particular, one must remember the rather rapid heating rate employed in the neutron experiment, and the rather large sample size, which may induce some thermal inertia. For the purpose of direct comparison, the experimental temperatures have been rescaled so as to bring the cubic–tetragonal transition points for the two sets into agreement.

Also the entropy excess data have been interpolated to obtain correlation between them and the order parameter data. The statistical error in entropy is negligible given the high number of experimental data points.

For every temperature point the values of ΔS are plotted against the values of the excess intensity from the neutron diffraction data, and the result is shown in figure 5. This graph shows that the two quantities are proportional to each other, indicating that this transition follows mean field Landau behaviour. The fit in figure 5 corresponds to the entire range of data collected for entropy, from just below T_c to around 30 K below T_c. The data points shown correspond to temperatures at which discrete measurements of the superlattice intensity have been made. Knowing now that a Landau potential may be used to describe this transition, we are able to analyse the excess entropy data in terms of such a model. While linear rescaling of temperature

for the neutron data has no effect on the thermodynamic character of the behaviour indicated, we note that this would add a small uncertainty to the accuracy of the derived parameters for the Landau coefficients.

It is important to note that it is necessary to check, by comparing the order parameter and entropy excess, whether this transition follows a mean field Landau theory or not, before analysing the entropy excess versus temperature in the framework of this theory.

Figure 4 shows that ΔS increases linearly below the transition temperature as the order parameter increases. At this point, the slope of ΔS versus temperature is a significant physical quantity. According to equation (3), in a 2–4 Landau potential, this slope gives a relation between coefficients A and B and we obtain, from figure 4, a value for $A^2/2B$ of 8.8×10^{-3} J K^{-2} mol^{-1}. For pure $SrTiO_3$, $A^2/2B = 7.8 \times 10^{-3}$ J K^{-2} mol^{-1} [15]. The two coefficients are of the same order of magnitude and this indicates that the cubic-to-tetragonal phase transition in the Ca-doped $SrTiO_3$, although far from the tricritical point, is strongly related to that in pure $SrTiO_3$.

Since the transition temperature, T_c, for a pure second-order phase transition can be shown to be equal to B/A we obtain a value of $A \approx 3.9$ J mol^{-1} K^{-1}, and $B \approx 850$ J mol^{-1}. Pure $SrTiO_3$ displays tricritical behaviour [15], with a much smaller value of B, and a larger value of C. The effect of addition of Ca into the structure on the transition behaviour is, therefore, to increase the effective transition temperature and move the system away from the tricritical point, with renormalization of the B-term of the Landau potential.

In this analysis we have not taken into account the quantum saturation shown in Q^2 because we are analysing a temperature interval near the transition where this effect can be neglected.

5. Conclusions

The cubic–tetragonal phase transition in 4% Ca-doped $SrTiO_3$ perovskite is, thermodynamically, second order, and further from tricritical than in pure $SrTiO_3$. The transition temperature, T_c, is significantly higher than in pure $SrTiO_3$. Both these observations may be understood in terms of the increase in the coefficient of the fourth-order term in the Landau potential. The order parameter obtained by means of neutron diffraction and the transition entropy excess correlate linearly, following Landau predictions. The entropy excess is linear with temperature down to at least 30 K below the transition temperature, and its slope gives relations between Landau coefficients similar to those obtained for pure $SrTiO_3$. Following equation (2), both the transition temperature and the specific heat excess increase with respect to those of pure $SrTiO_3$, which is compatible with Landau theory.

References

[1] Putnis A 1992 *Introduction to Mineral Sciences* (Cambridge: Cambridge University Press) pp 260, 404
[2] Redfern S A T 1996 *J. Phys.: Condens. Matter* **8** 8267
[3] Rajeev R and Pandey D 1999 *J. Phys.: Condens. Matter* **11** 2247
[4] Kennedy B J, Howard C J and Chakoumakos B C 1999 *J. Phys.: Condens. Matter* **11** 1479
[5] Galasso F S 1969 *Structure, Properties, and Preparation of Perovskite Type Compounds* (Oxford: Pergamon)
[6] Sleight A W, Gillson J L and Bierstedt P E 1975 *Solid State Commun.* **17** 27

[7]   Fontcuberta J, Martínez B, Seffar A, Pinol S, García-Munoz J L and Obradors X 1996 *Phys. Rev. Lett.* **76** 1122

[8]   Buttner R H and Maslen E N 1992 *Acta Crystallogr.* B **48** 639

[9]   Unoki H and Sakudo T 1967 *J. Phys. Soc. Japan* **23** 546
      Shapiro M, Axe J D and Shirane G 1972 *Phys. Rev.* B **6** 4332

[10] Bianchi U, Kleemand W and Bednorz J G J 1994 *J. Phys.: Condens. Matter* **6** 1229

[11] Guzhva M E, Markovin P A and Kleemann W 1997 *Phys. Solid State* **39** 625

[12] Becerro A I, Redfern S A T and Seifert F, to be submitted

[13] Qin S, Becerro A I, Seifert F, Gottsmann J and Jiang J 2000 *J. Mater. Chem.* **10** 1609

[14] Hayward S A and Salje E K H 1998 *J. Phys.: Condens. Matter* **10** 1421

[15] Salje E K H, Gallardo M C, Jiménez J, Romero F J and del Cerro J 1998 *J. Phys.: Condens. Matter* **10** 5535

[16] Martín-Olalla J M, Romero F J, Ramos S, Gallardo M C, Pérez-Mato J M and Salje E K H 2002 *J. Phys.: Condens. Matter* submitted

[17] del Cerro J 1989 *J. Phys. E: Sci. Instrum.* **20** 609

[18] Gallardo M C, Jiménez J and del Cerro J 1995 *Rev. Sci. Instrum.* **66** 5288

[19] Jiménez J, Rojas E and Zamora M 1984 *J. Appl. Phys.* **56** 3353

[20] del Cerro J, Romero F J, Gallardo M C, Hayward S A and Jiménez J 2000 *Thermochim. Acta* **343** 89

[21] Glazer A M 1972 *Acta Crystallogr.* B **28** 3384

[22] Carpenter M A 1992 Thermodynamics of phase transitions in minerals: a macroscopic approach *Stability of Minerals* ed G D Price and N L Ross (London: Chapman and Hall)

[23] Woodfield B F, Shapiro J L, Stevens S, Boerio-Goates J, Putnam R L, Helean K B and Navrotsky A 1999 *J. Chem. Thermodyn.* **31** 1573